Journal of Alloys and Compounds 509 (2011) 9549–9557

Contents lists available at ScienceDirect

Journal of Alloys and Compounds

journal homepage: www.elsevier.com/locate/jallcom

Mass transfer modeling on the separation of tantalum and niobium from dilute hydrofluoric media through a hollow fiber supported liquid membrane

Duenphen Buachuang[a], Prakorn Ramakul[b], Natchanun Leepipatpiboon[c], Ura Pancharoen[a,*]

[a] Department of Chemical Engineering, Faculty of Engineering, Chulalongkorn University, Bangkok 10330, Thailand
[b] Department of Chemical Engineering, Faculty of Engineering and Industrial Technology, Silpakorn University, Nakhon Pathom 73000, Thailand
[c] Chromatography and Separation Research Unit, Department of Chemistry, Faculty of Science, Chulalongkorn University, Patumwan, Bangkok 10330, Thailand

ARTICLE INFO

Article history:
Received 26 May 2011
Received in revised form 22 July 2011
Accepted 24 July 2011
Available online 29 July 2011

Keywords:
Flux
Hollow fiber
Liquid membrane
Modeling
Niobium
Tantalum

ABSTRACT

The separation of a mixture of tantalum and niobium in dilute hydrofluoric media via hollow fiber supported liquid membrane (HFSLM) was examined. Quaternary ammonium salt (Aliquat336) diluted in kerosene was used as a carrier. The various effects on the transport and separation of tantalum and niobium were studied: concentration of hydrofluoric acid in the feed solution, concentration of the carrier (Aliquat336) in the membrane phase, types of stripping solutions ($NaClO_4$, thiourea and HCl) and their concentration. The extraction of tantalum in the membrane phase from 0.3 M hydrofluoric acid (HF) by 3% (v/v) Aliquat336 was achieved by leaving niobium in the feed solution. Quantitative recovery of tantalum was achieved by 0.2 M $NaClO_4$. Furthermore, a mathematical model focusing on the extraction side of the liquid membrane system was presented in order to predict the concentration of tantalum at different times. The mass transfer coefficients of the aqueous feed (k_i) and the organic membrane phase (k_m) were estimated as 1.19×10^{-5} and 1.39×10^{-7} cm/s, respectively. Therefore, the mass transfer limiting step is the diffusion of tantalum–Aliquat336 through the liquid membrane. Moreover, mass transfer modeling was performed and the validity of the developed model evaluated. Experimental data and theoretical values were found to be in good agreement when the concentration of Aliquat336 in the membrane phase was below 4% (v/v).

1. Introduction

Tantalum and niobium usually occur together in nature. Both elements are deposited in various ores such as columbite, tantalite, tapiolite, pyrochlore, microlite and euxenite [1]. Because of their similar chemical properties, separation of the two elements is difficult. Consequently, their efficient separation and purification is of great importance, due to their promising applications in various industries. In addition, the industrial demand for both elements is continuously increasing [2,3]. Niobium is a good conductor of heat and electricity, has a high melting point, and resists corrosion. Accordingly it is widely used as an alloy element in super alloys for application in jet engine components. Tantalum is widely used in the electronics industry, mainly in capacitors, because its melting point is very high (3000 °C) and it has good corrosion resistance. Therefore, it is also used in aerospace structures, such as jet engine components, as well as in equipment in the chemical industry such as heat exchangers, evaporators, pumps, pipelines and tanks [4].

Many research studies have dealt with the separation and purification of these two elements. Most techniques have used liquid–liquid extraction, and a few have used a supported liquid membrane by using various extractants and mineral acid media. The separation of niobium from tantalum in chloride media has been achieved using tributylphosphate (TBP) and a synergistic mixture of TBP and Alamine 336 as carriers through a supported liquid membrane; this technique attained about 55% extraction of niobium, as reported by Campderrós and Marchese [5,6]. Mayorov and Nikolaev [7] performed liquid–liquid extraction for the purification of tantalum and niobium from fluoride–sulfuric acid media using octanol as a carrier. The result obtained completely separated tantalum from niobium at low acidity. Furthermore, Agulyansky et al. [8] achieved separation of tantalum and niobium in fluoride–sulfuric acid media with liquid–liquid extraction by using 2-octanol as an extractant in a multistage process. About 80% of the tantalum was extracted, but niobium was poorly extracted. Htwe and Lwin [9] extracted columbite–tantalite with a liquid–liquid extraction process using methyl isobutyl ketone (MIBK) in an HF–H_2SO_4 system, and recovered niobium using sulfuric acid solution as stripping.

In all the aforementioned literature, the separation of niobium and tantalum was successful using either a liquid–liquid extraction process, or (in a few cases) a flat sheet supported liquid

* Corresponding author. Tel.: +66 2218 6891; fax: +66 2218 6877.
E-mail address: ura.p.@chula.ac.th (U. Pancharoen).

0925-8388/$ – see front matter © 2011 Elsevier B.V. All rights reserved.
doi:10.1016/j.jallcom.2011.07.078

membrane. Recently, a supported liquid membrane process has become an attractive alternative to liquid–liquid extraction for metal separation because it can overcome the shortcomings of the traditional solvent extraction process: for example, emulsification, flooding, phase disengagement, large solvent inventory, and solvent evaporation [10]. Furthermore, there are various types of supported liquid membrane, including flat-plate type (FLM), spiral type, and hollow fiber supported liquid membrane (HFSLM), which is comprised of three phases: namely feed, organic, and stripping phases. The organic phase is a carrier which is embedded in the pores of the membrane, supported by capillary forces [11]. The organic phase contacts both feed and stripping phases. The target ions which dissolve in the feed phase then diffuse to the feed/membrane interface, react with the carrier to form a complex compound, and diffuse through the membrane to the membrane/stripping interface. They are then back-extracted by reacting with the stripping agent. Finally, the target ions are released into the stripping solution. Of the several types of SLM, a hollow fiber supported liquid membrane is the most promising. It possesses several advantages over a traditional solvent extraction method, such as simultaneous one-step extraction and stripping, high selectivity [12,13], low extractant and energy consumption, low capital and operating cost [14], large surface area to volume ratio, high mass transfer rate, no flooding [15], and easy scale-up [16]. For these reasons, HFSLM has been widely investigated for application in various fields: for instance, water treatment [17], and recovery of precious metals [18], rare earth metals [19] and radioactive metals [20] by using commercial extractants. In recent years, there have been no reports relating to the separation of tantalum and niobium using HFSLM. Because of the aforementioned advantages, the HFSLM process is promising for application in separating tantalum and niobium.

Aliquat336, a quaternary ammonium salt, is a stronger extractant than tertiary or secondary amines; the arrangement is $R_4N^+ > R_3NH^+ > R_2NH_2^+ > RNH_3^+$ [16]. It has been shown to be efficient in extracting various metals, e.g. arsenic (V) [21], cobalt (V) [22] and rhodium (III) [23]. Hence, it is a promising extractant for use in separating niobium and tantalum in a HFSLM process.

This work investigates the separation of tantalum and niobium from dilute hydrofluoric acid (HF) media, using Aliquat336, a quaternary ammonium salt, dissolved in kerosene as a carrier. The study focuses on optimizing the chemical condition to separate tantalum and niobium from their mixture. Several parameters were investigated, such as concentration of hydrofluoric acid (HF) in feed solution, concentration of Aliquat336, and types and concentrations of stripping agents. Additionally, we studied the modeling of this process. A model was presented to describe the transport mechanism through HFSLM. The mass transfer coefficient of the aqueous feed (k_i) and membrane phase (k_m) were estimated, and the rate-limiting step was found. Eventually, the theoretical values from the model were compared with experimental data.

2. Theory

The HFSLM system consists of a feed phase, organic membrane phase and stripping phase. The feed phase and stripping phase were in contact with the organic membrane phase. The organic membrane phase consisted of carriers embedded in porous material to enhance separation. The transport mechanism of metal ion is so-called "couple facilitated counter-transport," as shown in Fig. 1. The concentration gradient of ClO_4^- is the driving force of this process. The perchlorate ion is counter transport with tantalum ion. The target metal ion (TaF_7^{2-}) diffuses from the bulk feed phase through the stagnant layer of the feed side to arrive at the feed/membrane interface and react with the extractant ($R_4N^+X^-$) to form a complex

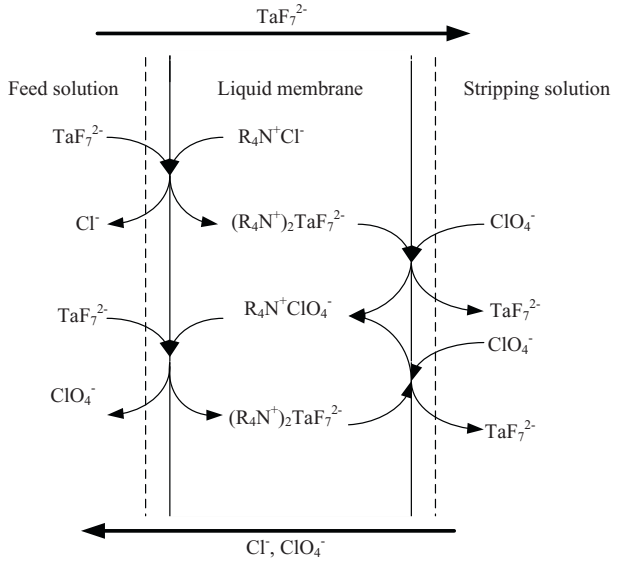

Fig. 1. Transport scheme of extraction and stripping in a liquid membrane process using Aliquat336 as an extractant.

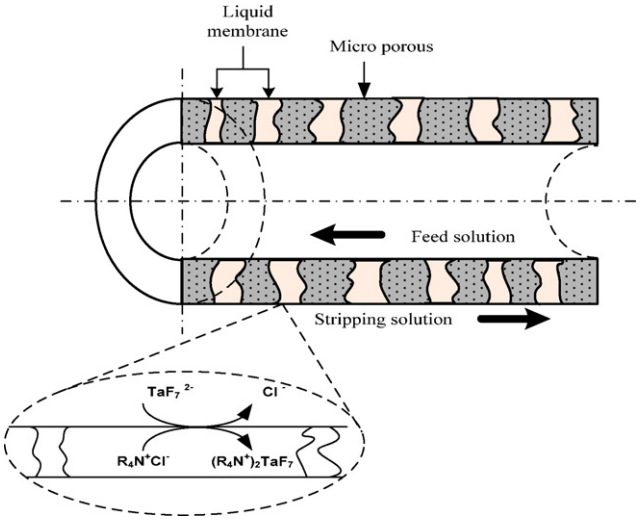

Fig. 2. Flow pattern in the hollow fiber supported liquid membrane module.

compound. X^- is denoted as Cl^- in feed and membrane phase in the first cycle, and ClO_4^- (a co-ion in the stripping phase) will replace Cl^- for the following cycle. Subsequently, the complex compound, $(R_4N)_2TaF_7^{2-}$, diffuses across the organic membrane phase to reach the membrane/stripping interface, where it reacts with the stripping agent (ClO_4^-). The target metal ion diffuses pass the stripping layer, while the extractant is regenerated by diffusing back to the feed/membrane interface. Lastly, the target ions are released to the stripping solution. The extraction and stripping reaction are shown in Eqs. (1) and (2), respectively.

The flow pattern in the HFSLM module consists of feed and stripping solutions, with countercurrent flows of feed solution in the tube side and stripping solution in the shell side, as illustrated in Fig. 2. The organic phase was filled in the pores of fibers by capillary force, acting as a barrier between the feed and stripping solutions. The extraction and stripping reactions occur at the interfaces (feed/membrane and membrane/stripping interface).

Tantalum and niobium have difference valences in a complex compound. Nevertheless, in a dilute HF solution, tantalum performs as an anionic complex of TaF_7^{2-} [8]. Methyltrioctylammonium

chloride (Aliquat336), a basic extractant, was a liquid membrane which was embedded in the hydrophobic microporous hollow fiber module. The extraction reaction of Aliquat336, $(R_4N^+)Cl^-$, with tantalum ions, TaF_7^{2-}, was according to Eq. (1):

$$TaF_7^{2-} + 2(R_4N^+Cl^-) \rightleftharpoons (R_4N)_2TaF_7 + 2Cl^- \quad (1)$$

The complex of tantalum ions–Aliquat336 diffused across the membrane phase to the opposite side due to the concentration gradient, and reacted with the stripping agent, ClO_4^-; then TaF_7^{2-} was released to the stripping solution. The stripping equation is shown in Eq. (2):

$$(R_4N)_2TaF_7 + 2NaClO_4 \rightleftharpoons 2(R_4N)ClO_4 + TaF_7^{2-} + 2Na^+ \quad (2)$$

TaF_7^{2-} ions were transferred to the stripping phase, whereas the extractant returned to the membrane phase and diffused to the feed–membrane interface due to the concentration gradient in order to react once again with TaF_7^{2-} in the feed solution.

The percentage of extraction and stripping were identified as follows:

$$\%\text{Extraction} = \frac{C_{f,in} - C_{f,out}}{C_{f,in}} \times 100 \quad (3)$$

$$\%\text{Stripping} = \frac{C_{s,out}}{C_{f,in}} \times 100 \quad (4)$$

where $C_{f,in}$ and $C_{f,out}$ are the inlet and outlet of metal concentration in the feed solution, and $C_{s,out}$ is the outlet of metal concentration in the stripping solution.

The extraction equilibrium constant K_{ex} of tantalum ions extracted by Aliquat336 in Eq. (1) was derived from the experimental data and determined using Eq. (5):

$$K_{ex} = \frac{[(R_4N)_2TaF_7][Cl^-]^2}{[TaF_7^{2-}][R_4N^+Cl^-]^2} \quad (5)$$

The distribution ratio of tantalum is shown in Eq. (6):

$$D = \frac{[(R_4N)_2TaF_7]}{[TaF_7^{2-}]} = \frac{K_{ex}[R_4N^+Cl^-]^2}{[Cl^-]^2} \quad (6)$$

The permeability coefficient (P), fast interfacial reactions, and the distribution of tantalum between the feed and membrane phase were calculated to be higher than those between the membrane and stripping phase. The equation for determining the permeability coefficient was expressed by Denesi [24]:

$$-V_f \ln\left(\frac{C_f}{C_{f,0}}\right) = AP\frac{\beta}{\beta+1}t \quad (7)$$

$$\beta = \frac{Q_f}{PL\varepsilon\pi Nr_i} \quad (8)$$

where P is the permeability coefficient (cm/s); V_f is the volume of the feed reservoir (cm^3); $C_{f,0}$ is the initial tantalum concentration (mol/L); C_f is the tantalum concentration at time t (mol/L); A is the effective area of the hollow fiber module (cm^2); t is time (min); Q_f is the volumetric flow rate (cm^3/s); L is the length of the hollow fiber (cm); ε is the porosity of the hollow fiber (%); N is the number of hollow fibers in the module; and r_i is the internal radius of the hollow fiber (cm).

The plot of $-V_f \ln(C_f/C_{f,0})$ as the function of t in Eq. (7) obtained $AP(\beta/\beta+1)$ as the slope; and P can be obtained by Eq. (8).

3. Experimental

3.1. Chemicals and reagents

All reagents used in this work – tantalum oxide (Ta_2O_5) and niobium oxide (Nb_2O_5) were purchased from Sigma–Aldrich (Germany) and Acros Organics/Fisher Scientific (USA), respectively. Aliquat336 (trioctylmethylammonium chloride) extractant was obtained from Sigma–Aldrich. The extractant was diluted in kerosene from Shell (Thailand). The structure of Aliquat336 is shown in Fig. 3. The reagents tested as stripping were NH_2CSNH_2 from QReC (New Zealand), and $NaClO_4$, analytical grade, from Acros Organics. Hydrofluoric acid (HF) analytical grade, used as acid media in feed solutions, was obtained from RFCL (India).

The stock solution of tantalum and niobium (1000 mg/L) was prepared by fusing tantalum oxide (Ta_2O_5) or niobium oxide (Nb_2O_5) with potassium bisulfate ($KHSO_4$) in a ratio of 20:1 by weight at 800 °C for 60 min. The melt was dissolved in 4% solution of ammonium oxalate [$(NH_4)_2C_2O_4{\cdot}H_2O$]. Feed solutions with various initial hydrofluoric acid (HF) concentrations were then prepared from this stock solution by proper dilution with deionized water and HF.

Table 1
Properties of the hollow fiber module.

Properties	Descriptions
Material	Polypropylene
Inside diameter of hollow fiber	240 μm
Outside diameter of hollow fiber	300 μm
Effective length of hollow fiber	15 cm
Number of hollow fibers	10,000
Pore size	0.03 μm
Porosity	25%
Effective surface area	1.4×10^4 cm^2
Area per unit volume	29.3 cm^2/cm^3
Module diameter	6.3 cm
Module length	20.3 cm
Tortuosity factor	2.6

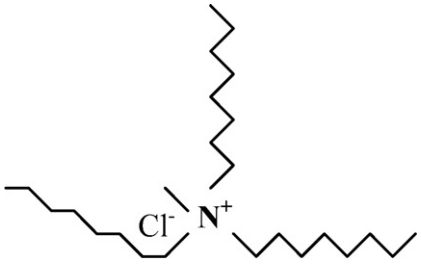

Fig. 3. Chemical structure of trioctylmethylammonium chloride (Aliquat336) [11].

3.2. Apparatus

The hollow fiber module (Liqui-Cel extra-flow module) was manufactured by Polypore (USA). This module uses Celgard microporous polyethylene fibers that are woven into fabric and wrapped around a central tube feeder that resembles a shell and tube configuration, with inlet/outlet ports for the shell and tube sides. The membrane is made from polypropylene, which is a hydrophobic material. The woven fabric provides more uniform fiber spacing, which in turn leads to a higher mass transfer coefficient than those obtained with individual fibers [25]. The properties of a hollow fiber module are listed in Table 1.

The hollow fiber module system is composed of two gear pumps, two variable-speed controller, two rotameters, and two pressure gauges. The system used in this study is displayed in Fig. 4.

3.3. Analytical instrument

Tantalum and niobium concentrations were determined using an inductively coupled plasma spectrometer (ICP-AES) (Perkin Elmer, USA).

3.4. Procedure

Batch system operation using a single module is shown in Fig. 4. The liquid membrane was prepared by dissolving Aliquat336 in 500 ml kerosene. This was slowly circulated in the lumen and shell sides of the module for 50 min to ensure that the extractant was entrapped in the micropores of hollow fibers. The experiment began by flowing the synthetic feed solution into the lumen side, whereas the stripping solution was fed counter-currently into the shell side. Flow rates on both sides were controlled to keep them equal, and circulation mode operation was performed. The system was carried out at room temperature (25 °C). The concentration of tantalum and niobium in the synthetic feed solution was equal to 10 mg/L. The concentration of HF in the feed solution was varied to attain the separation of tantalum and niobium. The concentration of Aliquat336 in the liquid membrane, and types and concentrations of stripping solution were investigated. The operating time for each experiment was 50 min. The concentration of tantalum and niobium ions in samples

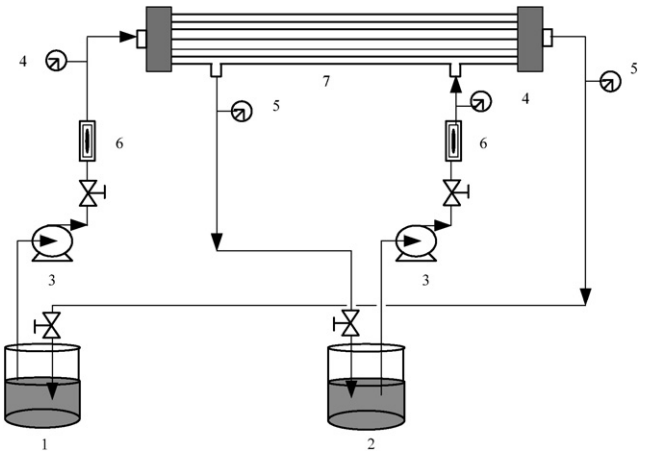

Fig. 4. Schematic counter-current flow diagram for a single-module operation in the HFSLM: (1) feed reservoir; (2) stripping reservoir; (3) gear pumps; (4) inlet pressure gauges; (5) outlet pressure gauges; (6) flow meter; (7) hollow fiber module.

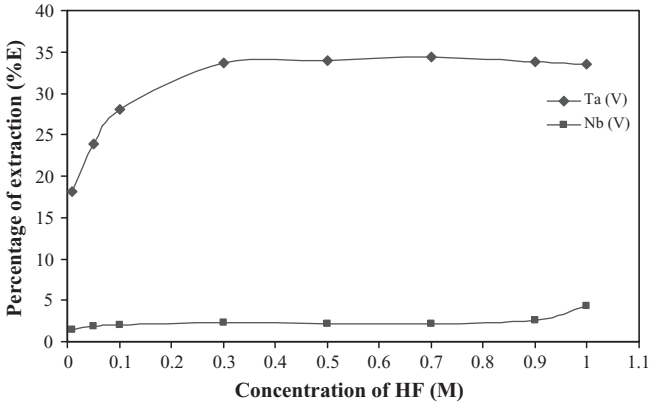

Fig. 5. Percentage of extraction against HF concentration of feed solution: 1% (v/v) Aliquat336 in kerosene, 10 ppm Ta and Nb in the feed solution, and 0.1 M NH_2CSNH_2 in the stripping solution. Flow rates of the feed and stripping solutions were 100 ml/min.

of feed and stripping solutions, taken from outlets on both sides, were analyzed by ICP to estimate the percentage of extraction and stripping.

4. Results and discussion

4.1. Effect of hydrofluoric acid concentration in the feed phase

The influence of HF concentration in the feed solution on the percentage of extraction of tantalum and niobium were studied in the range of 0.01–1 M. The results are shown in Fig. 5. At low concentrations of HF, poor extraction of niobium was observed. It was observed that the concentration of HF in the feed phase has a strong effect on selective extraction of tantalum over niobium. For this reason, an appropriate concentration of HF is necessary for the formation of an anionic complex of tantalum and niobium. The fluoro-tantalum complex is stronger compared to the fluoro-niobium complex [26]. At low HF concentration, tantalum performs as $[TaF_7]^{2-}$ [8,26], whereas the anion complex of niobium occurs when HF concentration is above 10 M, forming $[NbOF_n]^{3-n}$ or $[Nb(OH)_2F_n]^{3-n}$ (n = 2–6) [26]. Therefore, 0.3 M HF of feed solution is adequate to separate tantalum from niobium. The extraction reaction of tantalum is shown in Eq. (1).

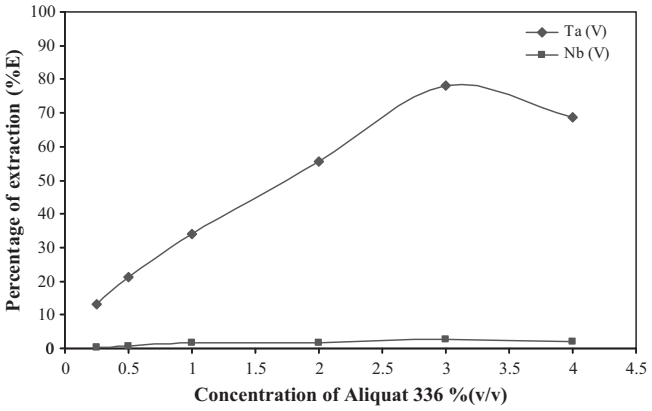

Fig. 6. Percentage of extraction against Aliquat336 concentration in the liquid membrane: 0.3 M HF, 10 ppm Ta and Nb in the feed solution, and 0.1 M H_2CSNH_2 in the stripping solution. Flow rates of the feed and stripping solutions were 100 ml/min.

4.2. Effect of carrier concentration in liquid membrane phase

The effect of carrier concentration on the percentage of extraction was studied. The experiments were performed for different Aliquat336 concentrations, ranging from 0.25 to 4% (v/v) in the membrane phase. The results are presented in Fig. 6. The concentration of Aliquat336 plays an important role in the percentage of extraction of metal ions in the feed solution. Increasing the Aliquat336 concentration from 0.25 to 3% (v/v) results in an increase in the percentage of extraction of tantalum. Nevertheless, a decrease in the percentage of extraction was observed for 4% (v/v) Aliquat336 concentration. It can thus be seen that increasing the concentration of Aliquat336 leads to increasing viscosity of the membrane phase; this obstructs diffusion, because viscosity and diffusivity are reversely correlated, by Eq. (9) [27]. The diffusion coefficient has a significant effect on the transport efficiency, and is associated with viscosity by the Stokes–Einstein equation. Increasing viscosity causes decreasing diffusivity and increases membrane phase resistance so that, in effect, it reduces the percentage of extraction, as in Eq. (9):

$$D^* = \frac{kT}{6\pi\eta r} \tag{9}$$

where D^* is the diffusion coefficient (cm^2/s), k is the Boltzmann constant, T is the absolute temperature, η is the viscosity of the organic phase, and r is the molecular radius of the solute (cm).

For Aliquat336 concentrations in a range of 0.25–3% (v/v), the percentage of extraction increases with increasing carrier concentration because of Le Chatelier's principle. From the results, 3% (v/v) Aliquat336 was selected as the optimum concentration, which attained a percentage of extraction of tantalum of about 80%.

4.3. Effect of types of stripping solution

In order to examine the effect of stripping agents on stripping efficiency, several different stripping types were used, such as $NaClO_4$, HCl, and thiourea, at identical concentrations of 0.1 M. The percentage of stripping by various stripping agents is presented in Fig. 7. It can be observed that the stripping efficiency for tantalum decreased in the order ClO_4^- > thiourea > Cl^-. Perchlorate was found to be the most efficient stripping agent, resulting from the higher anion lipophilicity and hydration free energy of perchlorate anions, as well as the large anions of perchlorate; hence it more easily dehydrated and more readily entered the membrane to facilitate transport [28]. In additional, the behavior of the reactant species can be explained by Lewis Acid–Base Theory (Hard and

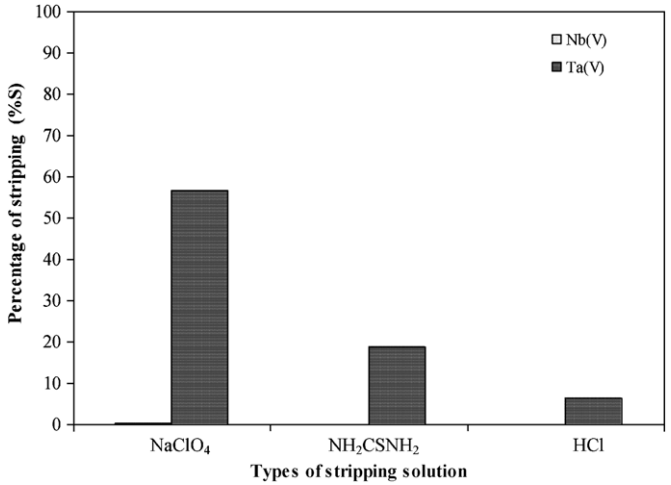

Fig. 7. Percentage of stripping by type of stripping solution: 3% (v/v) Aliquat336 in kerosene, 0.3 M HF, and 10 ppm Ta and Nb in the feed solution. Flow rates of the feed and stripping solutions were 100 ml/min.

Soft Acid/Base Theory). Thus, the cation of Aliquat336 is considered as a soft acid whereas Cl^- a hard base, ClO_4^- a soft base and NH_2CSNH_2 a very soft base. Therefore, the reaction between Aliquat336 and ClO_4^- species is favored in front of the other because both are soft. Perchlorate has been found to be a promising stripping agent, with indications that the tantalum–Aliquat336 complex can be decompounded by perchlorate. Whereas the niobium ion was poor extracted hence its stripping reaction was poor. Therefore, the subsequent experiments were carried out by using perchlorate as stripping solution.

4.4. Effect of stripping phase concentration

The influence of the concentration of $NaClO_4$ in the stripping phase was also studied. The concentration of $NaClO_4$ varied from 0.1 to 0.4 M. As seen in Fig. 8, a progressive increase in the percentage of tantalum stripping was found when the concentration of $NaClO_4$ increased up to optimum values of 0.2 M $NaClO_4$, which obtained the highest percentage of tantalum recovery (about 60%). At more than 0.2 M $NaClO_4$, it can be seen that the percentage of tantalum recovery was essentially constant.

The suggested mechanism for the transport of tantalum ions through the HFSLM is illustrated in Fig. 1. This couple facilitated counter-transport was achieved by the driving force of the

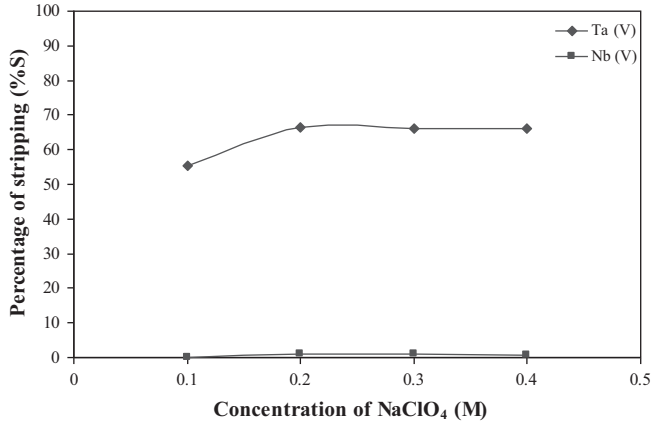

Fig. 8. Percentage of stripping against $NaClO_4$ concentration: 3% (v/v) Aliquat336 in kerosene, 0.3 M HF, and 10 ppm Ta and Nb in the feed solution. Flow rates of the feed and stripping solutions were 100 ml/min.

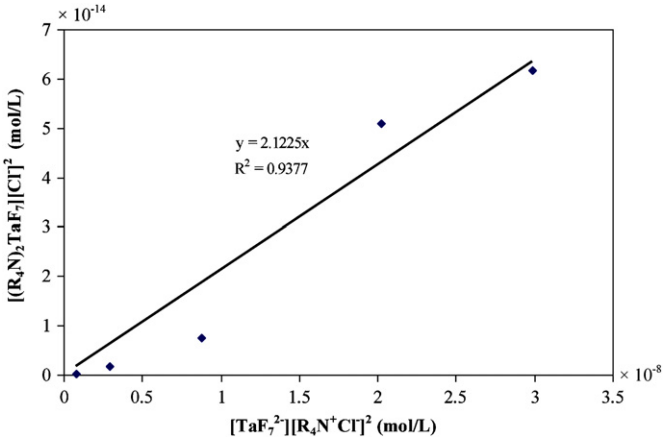

Fig. 9. The equilibrium constant: plot of $[(R_4N^+)_2TaF_7][Cl^-]^2$ and $[TaF_7^{2-}][R_4N^+Cl^-]^2$ at equilibrium for tantalum.

concentration gradient of $NaClO_4$. At the initial condition, in feed phase $NaClO_4$ was nil; while in stripping solution it varied in a range of 0.1–0.4 M. It was found that 0.2 M $NaClO_4$ was enough for the recovery of tantalum.

4.5. Extraction equilibrium constant and distribution coefficients

The extraction equilibrium constant of tantalum (K_{ex}) was estimated according to Eq. (5), by plotting of $[(R_4N^+)_2TaF_7][Cl^-]^2$ against $[TaF_7^{2-}][R_4N^+Cl^-]^2$ at equilibrium; the slopes obtained in Fig. 9 showed the equilibrium constant of tantalum (K_{ex}) as 2×10^{-6}. The distribution coefficients (D) of tantalum from the separation by HFSLM, presented in Table 2, were calculated by the linear curve in Fig. 9, using Eq. (6). It was observed that the distribution coefficient depended on the Aliquat336 concentration in the membrane phase. The distribution coefficient increased with increasing Aliquat336 concentration until reaching an optimum of 3% (v/v), and then decreased at Aliquat336 concentrations greater than 3% (v/v). This result can be explained by the increased Aliquat336 concentration resulting in sufficient carrier to extract tantalum into the membrane phase and diffuse it to the opposite side. On the other hand, at above the optimum point, the distribution coefficient of tantalum decreases due to the increase in viscosity of the organic phase with carrier concentration. In fact, increasing viscosity in the membrane phase leads to increased membrane resistance and difficulty in diffusion of the tantalum–carrier complex [29]. This result indicates that the Aliquat336 concentration should not exceed 3% (v/v).

4.6. Permeability coefficient

The permeability coefficients for tantalum separation at different Aliquat336 concentrations in the range of 0.25–4% (v/v) were calculated by the slopes obtained in Fig. 10, as shown in Table 2. It can be observed that permeability increases with carrier

Table 2
The distribution ratio (D) and the permeation coefficients (P) of tantalum at Aliquat336 concentrations of 0.25–4% (v/v).

Aliquat336 (% v/v)	D	$P \times 10^3$ (cm/s)
0.25	0.151	1.082
0.5	0.301	1.800
1	0.667	3.374
2	2.206	6.540
3	3.584	13.681
4	2.191	12.082

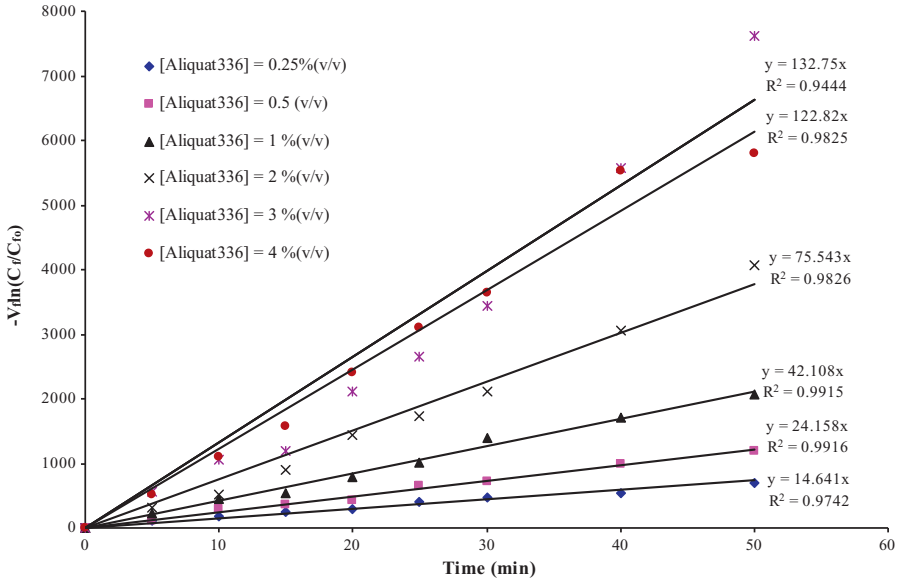

Fig. 10. Plot of $-V_f \ln(C_f/C_{f,0})$ of tantalum ions in the feed solution against time, with different Aliquat336 concentrations.

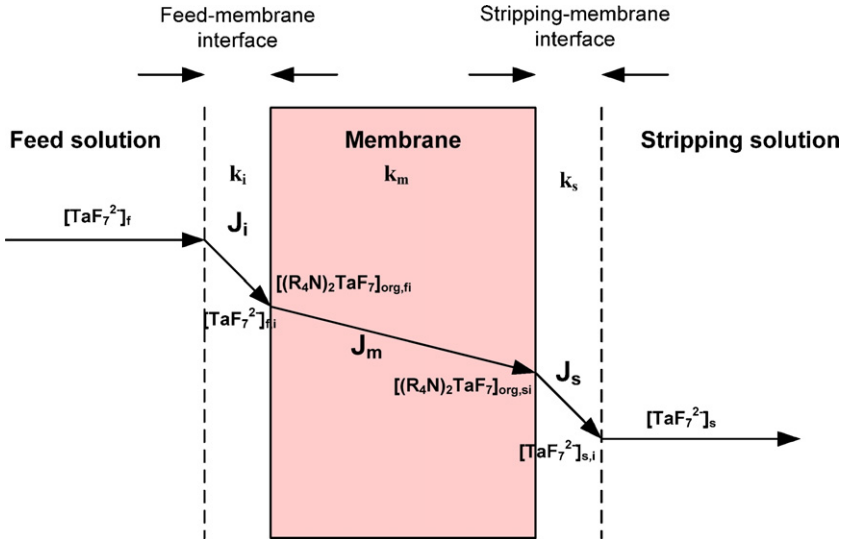

Fig. 11. Schematic representation of concentration profiles of tantalum transport through the HFSLM.

concentration until reaching optimum values, and then decreases. These results are similar to distribution coefficient values. The reason for the decrease of the permeability coefficient beyond 3% (v/v) Aliquat336 concentration was due to increasing viscosity in the membrane phase, as described in Section 4.2. In addition, the relationship of the permeation coefficient and viscosity is shown by the empirical Stokes–Einstein equation, Eq. (10) [30]:

$$P = \frac{kTK_f}{6\pi\eta r_s d} \tag{10}$$

where k is the Boltzmann constant, T is the absolute temperature, η is the viscosity of the organics phase, r_s is the molecular radius of the solute, d is the thickness of the membrane, K_f is the partition of the solute between the organic phase and feed phase, and P is the permeation coefficient.

4.7. Estimation of mass transfer coefficient

The main mass transfer rates through a hollow fiber supported liquid membrane are the diffusion steps. They are: the mass transfer coefficient of tantalum through the feed diffusion layer (k_i), the mass transfer coefficient of tantalum-carrier complexes through the organic phase (k_m), and the mass transfer coefficient of tantalum through the stripping diffusion layer (k_s), as shown in Fig. 11. Because the stripping reaction is instantaneous, the distribution of the stripping phase is neglected. It is noteworthy that k_s values are very high when compared with k_i and k_s values [31].

Theoretically, the flow through the tube side of a hollow fiber is laminar; hence the mass transfer coefficient of the feed phase (k_i) which flows in the tube side can be estimated based on the Sherwood–Graetz correlation [32]:

$$\mathrm{Gz} = \frac{d_i^2 v}{\mathrm{LD_{aq}}} \tag{11}$$

$$\mathrm{Sh} = \mathrm{mGz}^n \tag{12}$$

$$\mathrm{Sh} = \frac{k_i d_i}{D_{aq}} \tag{13}$$

where Sh and Gz are Sherwood and Graetz numbers, respectively; d_i is the inner diameter of fiber (cm); L is the length of fiber (cm); v is the linear velocity of the feed solution in the lumen side (cm/s); and D_{aq} is the diffusion coefficient of tantalum in the aqueous phase,

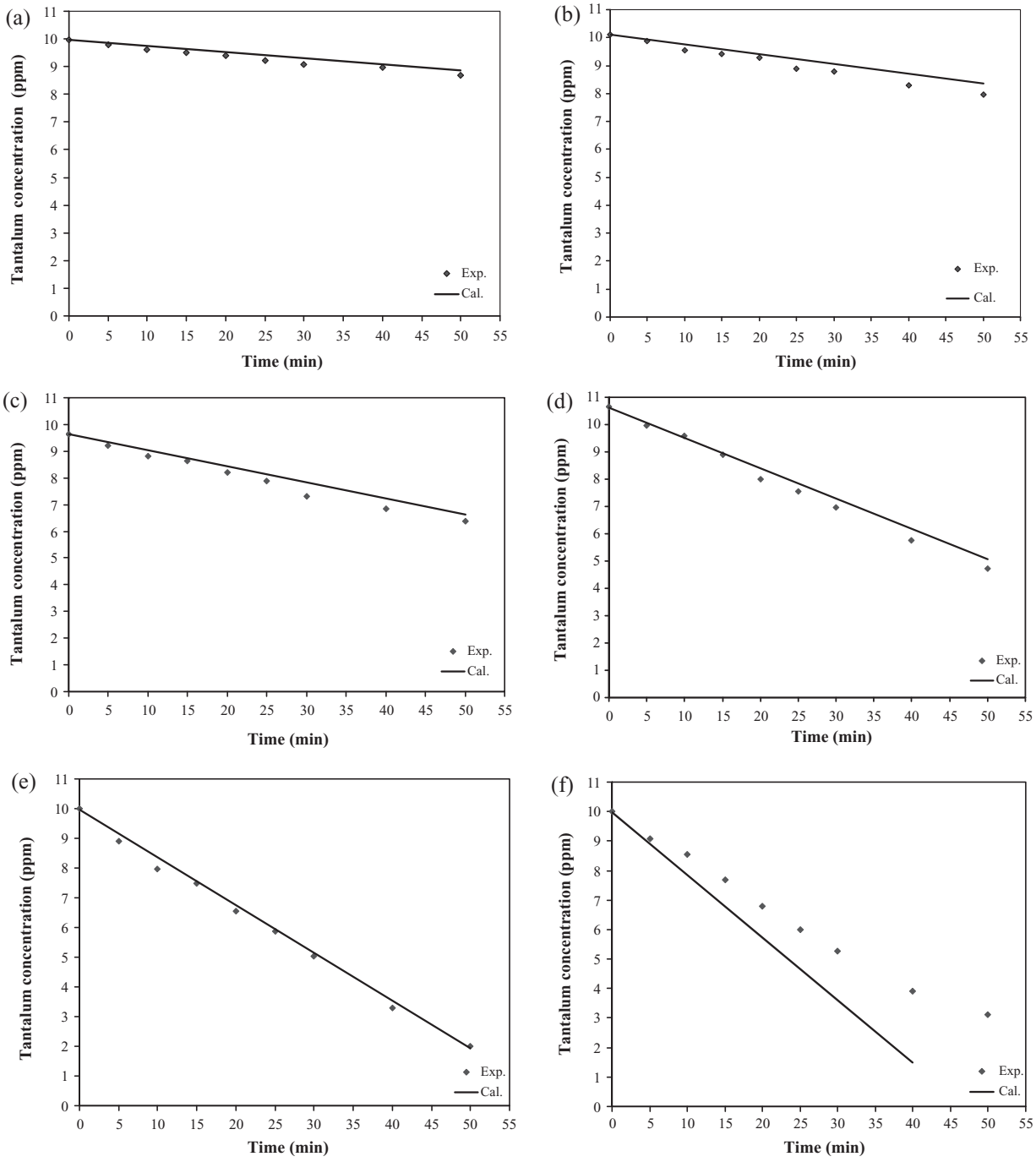

Fig. 12. Concentration of tantalum ions in the feed solution, plotted as a function of time at different concentrations of Aliquat336: (a) 0.25% (v/v); (b) 0.5% (v/v); (c) 1% (v/v); (d) 2% (v/v); (e) 3% (v/v); (f) 4% (v/v). Feed solution, 0.3 M HF and 10 ppm Ta and Nb; stripping solution, 0.2 M $NaClO_4$. Flow rates of the feed and stripping solutions were 100 ml/min. Symbols correspond to experimental values; the solid curve was calculated using Eq. (31).

which is estimated based on the Wilke–Chang equation [13], equal to 3.736×10^{-9} cm^2/s. Theoretically, for a diffusion process with fast chemical reaction $m = 1.62$, $n = 0.33$ approximate by Leveque [17,33]. The estimation of k_i from Sherwood–Graetz correlation is 1.19×10^{-5} cm/s.

The individual mass transfer coefficient in the membrane phase, k_m, can be approximated as follows [34]:

$$k_m = \frac{\varepsilon D_m}{\tau r_i \ \ln(r_o/r_i)} \tag{14}$$

where ε and τ are the porosity and tortuosity of the fiber membrane; D_m is the diffusivity of the tantalum–carrier complex in the membrane phase, 3.219×10^{-9} cm^2/s; and r_i and r_o are the internal and outer radii of the fiber (cm), respectively. The estimated k_m value is 1.39×10^{-7} cm/s.

The membrane mass transfer coefficient (k_m) is much less than the aqueous feed mass transfer coefficient (k_i). From these results, the mass transfer across the membrane phase is the rate-controlling step.

4.8. Mass transfer modeling of tantalum through a hollow fiber supported liquid membrane

The transportation and concentration profile of tantalum through HFSLM is shown in Fig. 11. The tantalum ions (TaF_7^{2-})

diffuse through the film layer of the feed phase towards the feed/membrane interface, where they instantly react with Aliquat336 to form a complex $(R_4N)_2TaF_7$). The complex diffuses across the membrane phase to reach the membrane/stripping interface, where de-complexing of $(R_4N)_2TaF_7$ occurs by reacting with perchlorate. Finally, TaF_7^{2-} diffuses through the stagnant layer of the stripping phase to the stripping solution. The diffusion process is explained by Flick's law. Mass transfer flux was presented in this model.

Consider the extraction reaction presented in Eq. (1). We denote that $[Ta]_{org}$ and $[Ta]_i$ are the concentrations of tantalum in the organic phase and at the interface between the feed and organic phases, respectively, where:

$$[Ta]_{org} = [(R_4N^+)_2TaF_7]_{org} \quad (15)$$

From Eq. (6), $[(R_4N^+)_2TaF_7]_{org,f}$ can be written in terms of the equilibrium constant as follows:

$$[Ta]_{org,f} = [(R_4N^+)_2TaF_7]_{org,f} = \frac{K_{ex}[(R_4N^+Cl^-)]^2}{[Cl^-]^2}[Ta]_{f,i} \quad (16)$$

The diffusion of the tantalum–carrier complex through the organic phase can be written as follows:

$$J_mR_m = [Ta]_{org,f} - [Ta]_{org,s} \quad (17)$$

where R_m = organic resistance results from diffusion through the membrane, and $[Ta]_{org,f}$ and $[Ta]_{org,s}$ are the concentrations of the tantalum–carrier complex at the feed/membrane and membrane/stripping interfaces, respectively.

The distribution of tantalum between the membrane and stripping phase is much less than that between the feed and membrane phase [35]. As a consequence, $[Ta]_{org,s}$ can be neglected. Therefore, Eq. (17) can be simplified to:

$$J_mR_m = [Ta]_{org,f} \quad (18)$$

The diffusion of tantalum from the bulk feed phase to the aqueous layer can be expressed by Flick's law as:

$$J_iR_i = [Ta]_f - [Ta]_{f,i} \quad (19)$$

where R_i is the aqueous phase resistance, and $[Ta]_f$ and $[Ta]_{f,i}$ are the concentrations of the tantalum complex in the feed solution and at the feed/membrane interface at time t, respectively.

The chemical reaction performed in Eq. (1) was considered to be fast compared to the diffusion rate. The reaction at the interface to reach equilibrium and the concentration at the interface are related by Eq. (16) [35]. Thus, $[Ta]_{org,f}$ from Eq. (16) was substituted in Eq. (18) to obtain:

$$[Ta]_{f,i} = \frac{J_mR_m[Cl^-]^2}{K_{ex}[R_4N^+Cl^-]^2} \quad (20)$$

At steady state, $J_m = J_i = J$, and by rearrangement of Eqs. (19) and (20), the expression for flux is obtained as follows:

$$J = \frac{K_{ex}[R_4N^+Cl^-]^2}{R_m[Cl^-]^2 + R_iK_{ex}[R_4N^+Cl^-]^2} \cdot [Ta]_f \quad (21)$$

The description of $[R_4N^+Cl^-]$ in the membrane phase is:

$$[R_4N^+Cl^-]_o = [R_4N^+Cl^-]_{free} + 2[Ta]_{org,f} \quad (22)$$

where $[R_4N^+Cl^-]_o$ is the initial concentration of Aliquat336 in the organic phase. When $[R_4N^+Cl^-]_o$ is low, it can be assumed that all of the Aliquat336 will react with tantalum ions. Hence, Eq. (22) can be rewritten as:

$$[R_4N^+Cl^-]_o \approx 2[Ta]_{org,f} \quad (23)$$

By combining and rearranging Eqs. (23) and (16), we obtain Eq. (24):

$$[R_4N^+Cl^-]^2 = \frac{[R_4N^+Cl^-]_0[Cl^-]^2}{2K_{ex}[Ta]_{f,i}} \quad (24)$$

Substituting Eq. (24) into Eq. (21), we have:

$$J = \frac{[R_4N^+Cl^-]_0}{2R_m[Ta]_{f,i} + R_i[R_4N^+Cl^-]_0} \cdot [Ta]_f \quad (25)$$

Due to the concentration of tantalum at the interface, ($[Ta]_{f,i}$) cannot be measured. Consequently, Eq. (19) was substituted and rearranged into a quadratic equation:

$$2R_mR_iJ^2 - (2R_m[Ta]_f + R_i[R_4N^+Cl^-]_0)J + [R_4N^+Cl^-]_0[Ta]_f = 0 \quad (26)$$

Therefore, the flux equation is obtained as:

$$J = \frac{2R_m[Ta]_f + R_i[R_4N^+Cl^-]_0 + \sqrt{(2R_m[Ta]_f + R_i[R_4N^+Cl^-]_0)^2 - 8R_mR_i[R_4N^+Cl^-]_0[Ta]_f}}{4R_mR_i} \quad (27)$$

because

$$\sqrt{(2R_m[Ta]_f + R_i[R_4N^+Cl^-]_0)^2 - 8R_mR_i[R_4N^+Cl^-]_0[Ta]_f} \ll 2R_m[Ta]_f + R_i[R_4N^+Cl^-]_0$$

so the term $\sqrt{(2R_m[Ta]_f + R_i[R_4N^+Cl^-]_0)^2 - 8R_mR_i[R_4N^+Cl^-]_0[Ta]_f}$ can be neglected and the overall flux expression obtained as follows:

$$J = \frac{[Ta]_f}{2R_i} + \frac{[R_4N^+Cl^-]_0}{4R_m} \quad (28)$$

with the definition of flux as:

$$J = \frac{-d[Ta]_f}{dt} \cdot \frac{V_f}{A} \quad (29)$$

where V_f and A are the volume of the feed reservoir (cm^3) and the effective area of the membrane (cm^2), respectively.

By combining Eqs. (28) and (29), we get:

$$\frac{-d[Ta]_f}{dt} \cdot \frac{V_f}{A} = \frac{[Ta]_f}{2R_i} + \frac{[R_4N^+Cl^-]_0}{4R_m} \quad (30)$$

Integrating Eq. (30) with initial condition $t = 0$ and $[Ta]_f = [Ta]_{f,o}$, the final equation for estimating tantalum concentration in feed solution can be expressed as:

$$[Ta]_f = \frac{-[R_4N^+Cl^-]_0R_i}{2R_m} + \left\{[Ta]_{f,o} + \frac{[R_4N^+Cl^-]_0R_i}{2R_m}\right\} \times \exp\left(\frac{-A}{2R_iV_f} \cdot t\right) \quad (31)$$

Fig. 12(a–f) illustrates the comparison of concentrations of tantalum from experimental data and theoretical values estimated using Eq. (31). The results indicate that when the concentration of Aliquat336 was lower than 4% (v/v), the mass transfer model was satisfactory, as demonstrated in Fig. 11(a–e). Nevertheless, when the concentration of Aliquat336 was more than 3% (v/v), the mass transfer model was poor. This error is likely due to the

assumption that the initial concentration of Aliquat336, $[R_4N^+Cl^-]_0$ is low and all of the Aliquat336 molecule will react with tantalum ions. So, when the concentration of Aliquat336 is higher than 3% (v/v), the liquid membrane's viscosity is very high. It obstructs the mass transfer and the metal-complex is accumulated in the liquid membrane. Moreover, the free Aliquat336 molecule is difficult to transport to react with tantalum ion. Therefore, the higher than 3% (v/v) of Aliquat336 brings the system to be out of the assumption.

5. Conclusions

Tantalum ions were purely extracted from niobium by HFSLM. The best conditions were 0.3 M HF, 3% (v/v) Aliquat336 and 0.2 M $NaClO_4$ of stripping solution, which resulted in the highest percentage of extraction and stripping of tantalum at optimal conditions (about 78% and 66%, respectively). The mass transfer coefficients of the aqueous feed phase (k_i) and membrane phase (k_m) were 1.19×10^{-5} and 1.39×10^{-7} cm/s, respectively. The mass transfer controlling step is the diffusion of tantalum–Aliquat336 through the organic membrane phase. Mass transfer modeling fit well with the experimental data when the concentration of Aliquat336 was lower than 4% (v/v).

Acknowledgements

The authors greatly appreciate financial support by the Thailand Research Fund (TRF) and the 90 anniversary of Chulalongkorn University Fund (Ratchadaphiseksomphot Endowment Fund) as well as Commission on Higher Education. We also wish to thank: the Separation Laboratory, Department of Chemical Engineering, Faculty of Engineering, Chulalongkorn University, for chemical and apparatus support; the Department of Chemical Engineering, Faculty of Engineering and Industrial Technology, Silpakorn University; and the Rare Earth Research and Development Center, Office of Atoms for Peace, Bangkok, Thailand, for the measurement of concentrations of tantalum and niobium by ICP.

References

[1] R.J.H. Clark, D. Brown, The Chemistry of Vanadium, Niobium and Tantalum, 1st ed., Pergamon Press, New York, 1975.
[2] E.G. Polyakov, L.P. Polyakova, Metallurgist 47 (2003) 33–41.
[3] N.I. Kasikova, A.G. Kasikov, G.V. Korotkova, Russ. J. Appl. Chem. 83 (2010) 424–429.
[4] L.D. Cunningham, U.S. Geological Survey Minerals Yearbook, USGS, Reston VA, 2000, pp. 1–7.
[5] M.E. Campderrós, J. Marchese, J. Membr. Sci. 164 (2000) 205–210.
[6] M.E. Campderrós, J. Marchese, Hydrometallurgy 61 (2001) 89–95.
[7] V.G. Mayorov, A.I. Nikolaev, Hydrometallurgy 66 (2002) 77–83.
[8] A. Agulyansky, L. Agulyansky, V.F. Travkin, Chem. Eng. Process. 43 (2004) 1231–1237.
[9] H.H. Htwe, K.T. Lwin, Eng. Technol. 36 (2008) 133–135.
[10] M. Teramoto, H. Matsuyama, H. Takaya, S. Asano, Sep. Sci. Technol. 22 (1987) 2175–2201.
[11] J. Lezamiz, J.Å. Jönsson, J. Chromatogr., A 1152 (2007) 226–233.
[12] W. Zhang, C. Cui, Z. Ren, Y. Dai, H. Meng, Chem. Eng. J. 157 (2010) 230–237.
[13] Q. Yang, N.M. Kocherginsky, J. Membr. Sci. 297 (2007) 121–129.
[14] J. Marchese, M. Campderrós, Desalination 164 (2004) 141–149.
[15] S.A. Ansari, P.K. Mohapatra, D.R. Raut, V.C. Adya, S.K. Thulasidas, V.K. Manchanda, Sep. Purif. Technol. 63 (2008) 239–242.
[16] W. Zhang, C. Cui, Z. Hao, Chin. J. Chem. Eng. 18 (2010) 48–54.
[17] G.R.M. Breembroek, A. van Straalen, G.J. Witkamp, G.M. van Rosmalen, J. Membr. Sci. 146 (1998) 185–195.
[18] A.A. Amiri, A. Safavi, A.R. Hasaninejad, H. Shrghi, M. Shamsipur, J. Membr. Sci. 325 (2008) 295–300.
[19] P. Ramakul, T. Supajaroon, T. Prapasawat, U. Pancharoen, A.W. Lothongkum, J. Ind. Eng. Chem. 15 (2009) 224–228.
[20] P. Ramakul, T. Prapasawat, U. Pancharoen, W. Pattaveekongka, J. Chin. Inst. Chem. Eng. 38 (2007) 489–494.
[21] S. Bey, A. Criscuoli, A. Figoli, A. Leopold, S. Simone, M. Benamor, E. Drioli, Desalination 264 (2010) 193–200.
[22] H.-C. Kao, R.-S. Juang, J. Membr. Sci. 264 (2005) 104–112.
[23] C. Fontàs, C. Palet, V. Salvadó, M. Hidalgo, J. Membr. Sci. 178 (2000) 131–139.
[24] P.R. Danesi, C. Cianetti, J. Membr. Sci. 20 (1984) 201–213.
[25] Liqui-Cel. http://www.liqui-cel.com (accessed 28.04.11).
[26] R. Caletka, R. Hausbeck, V. Krivan, J. Radioanal. Nucl. Chem. 131 (1989) 343–352.
[27] S.K. Singh, S.K. Misra, S.C. Tripathi, D.K. Singh, Desalination 250 (2010) 19–25.
[28] V.S. Kislik, Carrier-Facilitated Coupled Transport Through Liquid Membranes: General Theoretical Considerations and Influencing Parameters, Liquid Membranes: Principles and Applications in Chemical Separations and Wastewater Treatment, Elsevier B.V., 2010, pp. 17–71.
[29] C. Zidi, R. Tayeb, M. Ben Sik Ali, M. Dhahbi, J. Membr. Sci. 360 (2010) 334–340.
[30] P. Dzygiel, P.P. Wieczorek, Supported Liquid Membranes and Their Modifications: Definition, Classification,Theory, Stability, Application and Perspectives, Liquid Membranes: Principles and Applications in Chemical Separations and Wastewater Treatment, Elsevier B.V., 2010, pp. 73–140.
[31] U. Pancharoen, S. Somboonpanya, S. Chaturabul, A.W. Lothongkum, J. Alloys Compd. 489 (2010) 72–79.
[32] N.M. Kocherginsky, Q. Yang, L. Seelam, Sep. Purif. Technol. 53 (2007) 171–177.
[33] M.A. Leveque, Les lois de la transmission de chaleur par convection, Ann. Mines Mem. Ser. 12–13 (1928) 201–239.
[34] R.-S. Juang, H.-L. Huang, J. Membr. Sci. 213 (2003) 125–135.
[35] K. Chakrabarty, P. Saha, A.K. Ghoshal, J. Membr. Sci. 340 (2009) 84–91.